

Article

# Exploring the mechanism of XieBai San in treating liver injury based on network pharmacology and experimental verification

Tingting Hou<sup>†</sup>, Chunjie Yang<sup>†</sup>, You Lv<sup>†</sup>, Yongfeng Ma, Runhua Li, Mingli Shang, Qianwen Zhang, Cheng Luo, Huiqin Qian\*, Xiaoyue Lou\*

College of Pharmacy, Sanquan College of Xinxiang Medical University, Xinxiang 453000, China

\* **Corresponding authors:** Xiaoyue Lou, 846749902@qq.com; Huiqin Qian, 14522009@sqmc.edu.cn

<sup>†</sup> Tingting Hou, Chunjie Yang and You Lv contributed equally to this work

## CITATION

Hou T, Yang C, Lv Y, et al.  
Exploring the mechanism of XieBai San in treating liver injury based on network pharmacology and experimental verification. *Molecular & Cellular Biomechanics*. 2024; 21(4): 864.  
<https://doi.org/10.62617/mcb864>

## ARTICLE INFO

Received: 21 November 2024  
Accepted: 16 December 2024  
Available online: 31 December 2024

## COPYRIGHT



Copyright © 2024 by author(s).  
*Molecular & Cellular Biomechanics* is published by Sin-Chn Scientific Press Pte. Ltd. This work is licensed under the Creative Commons Attribution (CC BY) license.  
<https://creativecommons.org/licenses/by/4.0/>

**Abstract:** The XieBai San (XBS) formula contains SangbaiPi (Cortex Mori), Digupi (Cortex Lycii), and Gancao (Radix Glycyrrhizae). Some studies have shown that XBS exerts a healing impact on liver damage. However, the specific active components and the underlying mechanism are still not fully understood. To explore this phenomenon, we administered a 0.2% CCl<sub>4</sub> oil solution to mice to elicit acute liver damage, and then XBS was given by gavage to mice. The results indicated that XBS exhibited a beneficial impact on liver injury. TCMSP, PubChem, SwissTargetPrediction, and GeneCards and DisGeNET databases were used to screen the active components of Cortex Mori, Cortex Lycii, and Radix Glycyrrhizae in XBS and their therapeutic targets for liver injury. Venn diagrams was utilized to identify the intersecting genes and the STRING database to explore protein-protein interactions. PPI networks and drug-component-target networks were constructed through Cytoscape software. Additionally, GO and KEGG enrichment studies were performed utilizing the DAVID platform. Subsequently, molecular docking validation was carried out using AutoDockTools version 1.5.6. The main active components of XBS were quercetin, jaranol, isorhamnetin, sitosterol, and kaempferol. The key targets were AKT1, EGFR, ESR1, PIK3CA, and PIK3R1. The predicted key targets were involved in positive regulation of peptide-bound serine phosphorylation and other biological processes that can restore liver function, anti-inflammatory response, and antioxidant stress to treat liver injury. XBS exerts its therapeutic effect on liver injury through multiple targets and mechanisms.

**Keywords:** network pharmacology; molecular docking; XieBai San (XBS); liver injury

## 1. Introduction

The liver stands as a pivotal organ in both human and animal bodies. The causes and treatments of liver injury have become the focus of current research [1]. Viral infection, autoimmune disease, trauma, and chemical substances can all cause liver injury, which can even deteriorate into cirrhosis and liver cancer and further be harmful to human health [2]. In recent years, traditional Chinese medicines have yielded notable achievements in the treatment of liver injury [3]. They can help eliminate inflammation, promote metabolism to treat liver injury, and effectively alleviate clinical symptoms and protect the liver [4]. Hence, discovering an efficacious traditional Chinese medicine for liver injury treatment holds immense importance.

XieBai San (XBS) contains SangbaiPi (Cortex Mori), Digupi (Cortex Lycii), and Gancao (Radix Glycyrrhizae) [5]. The Cortex Mori originates from the root bark of the mulberry tree, which belongs to the Moraceae family, and its components mainly consist of stilbenes, flavonoids, coumarins, aromatic benzofurans, N-carbohydrates,

and steroids. The components of Cortex Lycii, which is the root bark of *Lycium barbarum* and other plants in the Solanaceae family, mainly include organic acid compounds, octapeptides, diamides, alkaloids, and phenols [6]. Radix glycyrrhizae is derived from the roots and rhizomes of *Glycyrrhiza uralensis* Fisch. and contains liquiritin, glycyrrhizin, glycyrrhizin oxide, glycyrrhizin alcohol and other components. Studies have shown that XBS has a relevant effect in the treatment of liver injury, but the specific active components and the underlying mechanism by which it treats liver injury remain uncertain.

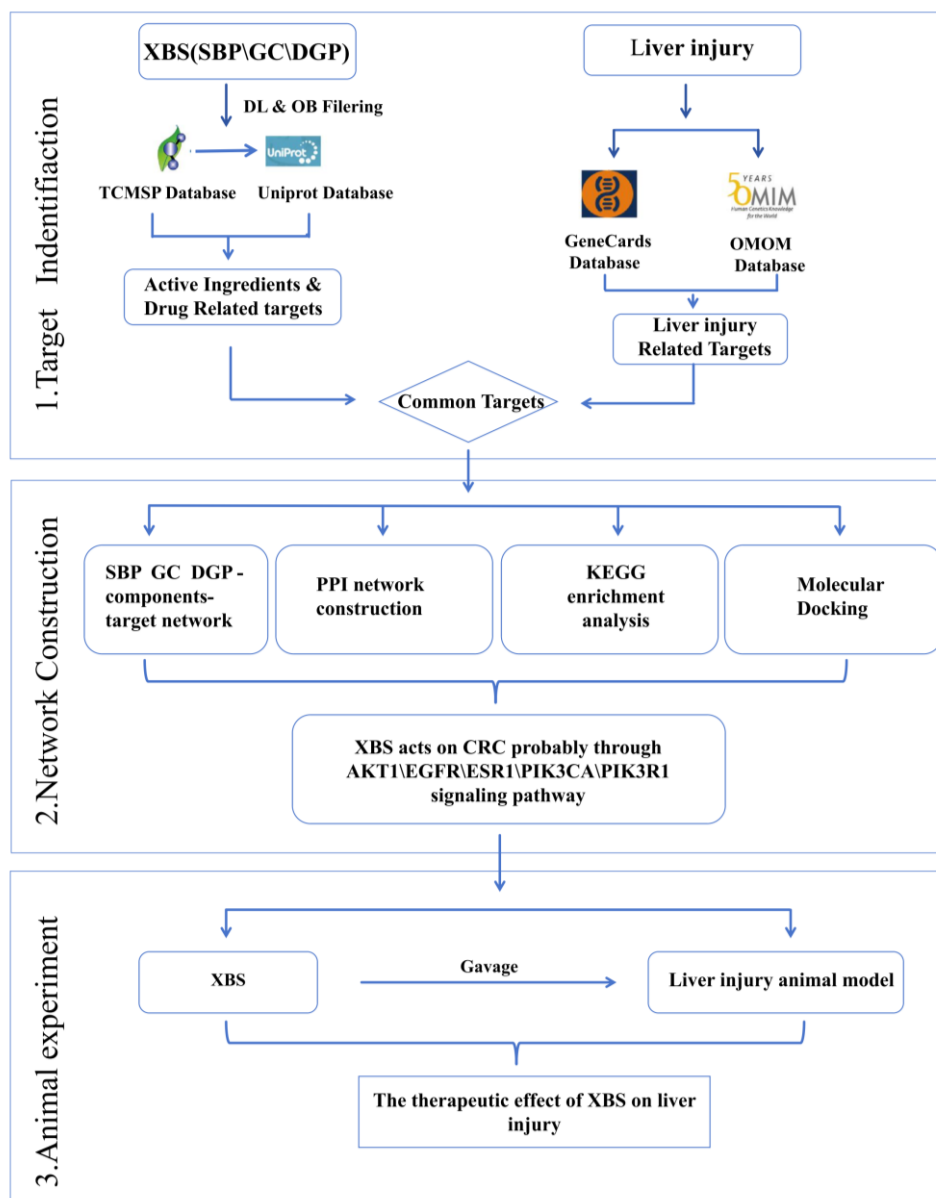


**Figure 1.** The workflow of the present study.

Network pharmacology involves exploring the mechanisms of action of TCM in treating diseases through multiple targets and pathways, by analyzing the targets of drugs and diseases. The core problem is to evaluate the comprehensive influence of the synergistic action of multiple targets of traditional Chinese medicine on the disease-related molecular network to systematically expound from the perspective of

component-target-pathway-disease [7]. Molecular docking is a drug design approach rooted in the interaction between receptors and drug molecules. As a theoretical simulation technique, it primarily focuses on studying the interaction between ligands and receptors, predicting their binding patterns and affinities. In recent years, molecular docking has emerged as a crucial tool in computer-aided drug research, playing a pivotal role in the fields of enzymology and pharmaceutical research.

According to the study, we used 0.2% CCl<sub>4</sub> oil solution to cause acute liver injury in mice, and administered XBS orally to the mice. We found that XBS has a pharmacological effect in treating liver injury. In addition, we investigated the efficacious constituents and putative molecular targets of XBS in therapeutic applications for liver injury through network pharmacology, and analyzed its potential mechanism. Finally, we confirmed the binding mode and affinity between molecules through molecular docking. The workflow of the current study is shown in **Figure 1**.

## **2. Materials and methods**

### **2.1. Reagents and chemicals**

Sodium carboxymethyl cellulose (Merck Life Sciences Ltd., Batch No. 023J5431); physiological saline (0.9% NaCl); bifendate (Wepon Pharmaceutical Group Co., Ltd., Batch No. 19J22123); alanine aminotransferase (ALT/GPT) test kit (colorimetric method) (Nanjing Jiancheng Biological Products, Batch No. 20230323); aspartate aminotransferase (AST/GOT) test kit (colorimetric method) (Nanjing Jiancheng Biological Products, Batch No. 20230917); 96-well cell culture plate (LABSELECT cell culture plate). Cortex mori (ZY2212045), Cortex lycii (ZY2212021), and Radix Glycyrrhizae (ZY2301050) were acquired from Beijing Tongrentang (Anguo) Traditional Chinese Medicine Pieces Co., Ltd. (Beijing, China).

### **2.2. Preparation of XBS**

The XBS is composed of three herbs, Cortex Mori, Cortex Lycii, and Radix Glycyrrhizae. 18 g Cortex Mori, 18 g Cortex Lycii, and 1.8 g Radix Glycyrrhizae, 0.3 g of glutinous rice were mixed, and 180 mL of distilled water was added into the mixture. It was then mixed with gently boiled for 40 min, then strained through a piece of gauze to obtain the filtrate. The filtrate was reduced to 31.75 mL at 60 °C–65 °C, yielding a final XBS concentration of 1.2 g/mL. The XBS solution was stored at 4 °C. According to the required concentration, the XBS solution was diluted to 0.3 g/mL, 0.6 g/mL, 1.2 g/mL, respectively.

### **2.3. Animals**

Kunming mice (male, 6–8 weeks old) were purchased from Beijing Vital River Laboratory Animal Technology Co., Ltd. in China and housed at Zhengzhou University School of Medical Sciences' Experimental Animal Platform. The experimental procedures were approved by the platform's Ethics Committee. The ethics approval number for this experiment is ZZU-LAC20230210. During the experiment, the mice had unrestricted access to water and food, and the environment was maintained at a temperature of 20 °C–25 °C and humidity of 50%–60%.

## **2.4. Animal experimental procedures**

After 7 days of adaptive feeding, 54 mice were randomly assigned to six groups (n = 9). Group A, the model group, received a standard dose of normal saline (0.1 mL/10 g). Group B is the blank control group mice received normal saline at a dose of 0.1 mL/10 g via gavage for 5 consecutive days; Group C is the positive drug group: mice were administered with the suspension of bifendate CMC-Na (200 mg/kg/d) via gavage for 5 consecutive days [8]; D, E, and F groups of mice were given XBS doses of 3 g/kg/d, 6 g/kg/d, and 12 g/kg/d via gavage for 5 consecutive days, respectively.

The model group of CCl<sub>4</sub> (Group A), the positive control group of bifendate (Group C), and the D, E, and F treatment groups were intraperitoneally injected with 0.2% CCl<sub>4</sub> glycerin solution (0.1 mL/10 g) 1 h after the fifth day of treatment to induce acute liver injury. The eyes were punctured for blood collection after 24 h, and the liver and spleen were collected.

## **2.5. Liver and spleen index analysis**

The Liver and spleen tissues were collected and weighed. Finally, the liver and spleen index were calculated using the following formula:

$$\text{Liver index} = \text{liver weight (g)} / \text{body weight (g)}$$

$$\text{Spleen index} = \text{spleen weight (g)} / \text{body weight (g)}$$

## **2.6. Detection indicators for liver injury**

The serum was collected for the analysis of alanine aminotransferase (ALT) and aspartate aminotransferase (AST) levels with related assay kits, according to manufacturers' instructions.

## **2.7. Collection of active ingredients**

TCMSP database (<http://tcmsp.w.com/tcmsp.php>), PubChem database (<https://pubchem.ncbi.nlm.nih.gov/>), and SwissTargetPrediction database (<http://swisstargetprediction.ch>) were used to collect potential active ingredients using  $OB \geq 30\%$  and  $DL \geq 0.18$  as screening conditions [9–11]. The qualified chemical components were obtained and their InChIkey were saved. In addition, relevant research contents were collected to supplement potential compounds in XBS [12].

## **2.8. Prediction of drug targets**

The InChIkeys from the TCMSP database for the drug's active ingredients were employed to perform searches in the PubChem database. The SMILES codes of the drug active ingredients were obtained. To predict the target proteins of the active ingredients of XBS, SwissTargetPrediction database (<http://swisstargetprediction.ch/>) was used. The SMILES codes retrieved from the PubChem database for the drug's active ingredient were input into the SwissTargetPrediction database, and the target proteins of the drug active ingredient were obtained.

## 2.9. Screening of common targets of drugs and diseases

The drug activity targets and liver injury targets identified through screening were imported into the Venny 2.1.0 platform (<https://bioinfogp.cnb.csic.es/tools/venny/index.html>), to identify the overlapping targets between the drugs in XBS and those associated with liver injury.

## 2.10. Construction of drug-component-target network diagram

Cytoscape 3.9.1 software was utilized to construct and analyze the drug-component-target network. The components whose Betweenness Centrality (BC), Closeness Centrality (CC) and Degree were both higher than the average value were selected, and the top five components were taken as core components [13].

## 2.11. Protein-protein interaction analysis (PPI) and visualization

The common gene targets were incorporated into the STRING (<https://stringdb.org/>) database, with a protein interaction threshold set at above 0.7. Cytoscape version 3.9.1 was utilized to build the protein-protein interaction (PPI) network. In this network, targets with a higher number of edges indicate greater significance [14]. The top five components with higher degree, BC, and CC than the average was seen as core targets [15].

## 2.12. GO function and KEGG pathway enrichment analysis

The DAVID (<https://david.ncifcrf.gov/>) database was employed to conduct Gene Ontology (GO) analysis and Kyoto Encyclopedia of Genes and Genomes (KEGG) signaling pathway enrichment analysis on the key targets. We selected the top 20 results with a *p*-value below 0.05 or lower for visualization in bubble or bar graphs. In the bubble map, smaller *p* values were represented by larger and darker bubbles.

## 2.13. Molecular docking verification and visualization of XBS

The three-dimensional structures of the core target proteins were obtained from the PDB database (<https://www1.rcsb.org/>), and preprocessed by PyMOL software, such as ligand removal and decoys. Crystal protein structures were obtained from the Protein Data Bank (<https://www.uniprot.org/>), and the details of the protein targets were as follows: EGFR (PDB ID: 5HG8), AKT1 (PDB ID: 1UNQ), PIK3R1 (PDB ID: 4JPS), PIK3CA (PDB ID: 7L1C), and ESR1 (PDB ID: 1XPC). AutoDockTools1.5.6 were used to perform hydrogenation and charge addition [16]. The binding energy  $\leq -5$  kcal/mol indicates good binding activity, and the binding energy  $\leq -7$  kcal/mol suggests strong binding activity between the compound and the target [17,18]. The results with good binding activity were imported into PyMOL for visualization.

## 2.14. Statistical analysis

All statistics were presented as mean  $\pm$  standard deviation. GraphPad Prism 9.0 and Excel software were used for statistics analysis. The differences were compared via one-way ANOVA among groups, and *p* < 0.05 were considered significant.

### 3. Results

#### 3.1. The therapeutic effect of XBS on CCl<sub>4</sub>-induced acute liver injury

The animal model of acute liver injury was established, and statistical variations in the liver and spleen indices were examined among different mouse groups. The liver and spleen indices in the model group exhibited significantly elevated levels compared to those in the control group ( $p < 0.0001$ ), while all of them were lower in middle dose, high dose, and positive medicine group compared to those in the model group ( $p < 0.0001$ ), as shown in **Figure 2**. When compared to the control group, the model group exhibited significantly heightened levels of AST and ALT. Furthermore, in comparison to the model group, XBS was found to dose-dependently decrease AST and ALT levels ( $p < 0.0001$ ). These findings provided compelling evidence for the therapeutic efficacy of XBS in treating CCl<sub>4</sub>-induced acute liver injury, as illustrated in **Figure 3**.

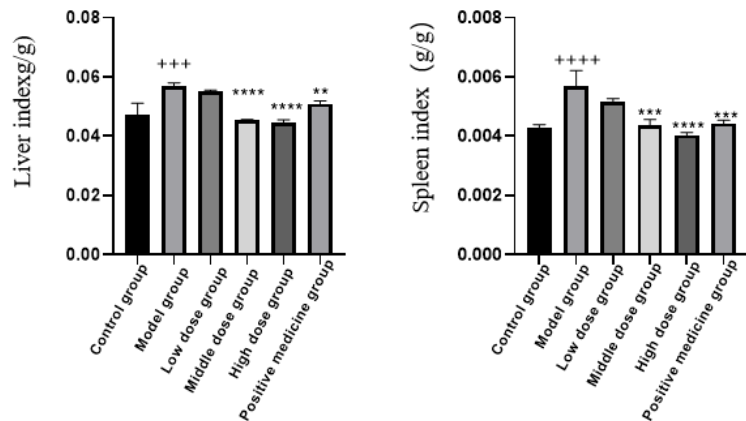


**Figure 2.** XBS reduced renal index and spleen index in mice with acute liver injury induced by CCl<sub>4</sub>.

Note:  $n = 9$ . Compared with the control group,  $++++ p < 0.0001$ ; compared with the model group,  $* p < 0.05$ ,  $** p < 0.01$ ,  $*** p < 0.001$ ,  $**** p < 0.0001$ .

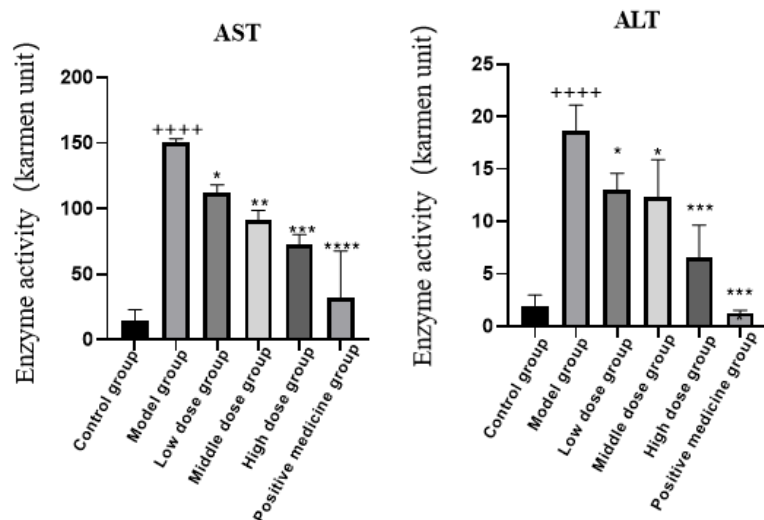


**Figure 3.** XBS reduced AST and ALT levels in acute liver injury induced by CCl<sub>4</sub>.

Note:  $n = 9$ .  $++++ p < 0.0001$  vs. control group;  $* p < 0.05$ ,  $** p < 0.01$ ,  $*** p < 0.001$ ,  $**** p < 0.0001$  vs. Model group.

### 3.2. Exploration of the main components of XBS

After screened in the TCMSP database, 32 active ingredients in Cortex Mori, 13 active ingredients in Cortex Lycii and 92 active ingredients in Radix Glycyrrhizae were collected and shown in **Table 1**. The details were presented in supplementary **Tables S1–S3**.

**Table 1.** Effective components screened from XBS.

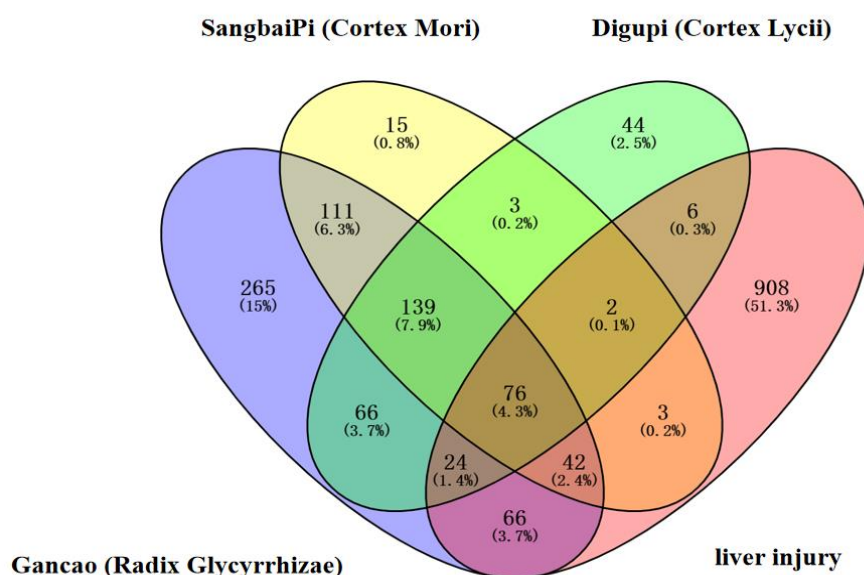
Drug	Mol ID	Molecule Name	OB (%)	DL
Cortex Mori	MOL012681	Dimethyl(methylenedi-4,1-phenylene) bis carbamate	50.84	0.26
	MOL012686	7-methoxy-5, 4'-dihydroxyflavanonol	51.72	0.26
	MOL012689	cyclomulberochromene	36.79	0.87
	MOL012692	kuwanonD	31.09	0.8
	MOL012714	MoracinA	64.39	0.23
Cortex Lycii	MOL001689	acacetin	34.97	0.24
	MOL002219	Atropine	34.53	0.21
	MOL002224	aurantiamide acetate	58.38	0.59
	MOL000358	beta-sitosterol	36.91	0.75
	MOL000953	CLR	37.87	0.68
	MOL000296	hederagenin	36.91	0.75
	MOL002228	Kulactone	45.44	0.82
	MOL001790	Linarin	39.84	0.71
	MOL001645	Linoleyl acetate	42.1	0.2
	MOL001552	OIN	45.97	0.19
	MOL002218	scopolin	56.45	0.39
	MOL000449	Stigmasterol	43.83	0.76
MOL002222	sugiol	36.11	0.28	
Radix Glycyrrhizae	MOL004993	8-prenylated eriodictyol	53.79	0.4
	MOL000417	Calycosin	47.75	0.24
	MOL005020	dehydroglyasperins C	53.82	0.37
	MOL001792	DFV	32.76	0.18
	MOL004806	euchrenone	30.29	0.57

### 3.3. Screening of XBS chemical ingredient targets and liver injury targets

Using SwissTargetPrediction, TCMSP, and Pubchem, we identified 391 targets for the active components of Cortex Mori, 360 targets for Cortex Lycii's active ingredients, and 789 targets for those in Radix Glycyrrhizae. Additionally, we retrieved 1128 disease-related targets from the GeneCards and DISGENET databases. 76 common gene targets were obtained using Venny diagram (**Table 2** and **Figure 4**).

**Table 2.** Intersection targets between XBS and liver injury.

Intersection target									
AR	CDC25B	CES2	UGT2B7	VDR	SERPINA6	G6PD	PPARG	TERT	
MDM2	PTGS2	NOX4	MCL1	ABCB1	ABCG2	FLT3	APP	PLG	
EGFR	KIT	XDH	NOS2	ESR1	AKT1	IGF1R	MMP9	MMP2	
ABCC1	AHR	F2	CDK1	GSK3B	MAOA	SRC	PTK2	KDR	
SYK	BCHE	CYP1A1	CYP1A2	CDK2	DRD4	MPO	PIK3R1	PYGL	
MMP3	CA3	ARG1	PARP1	TTR	MMP12	HMGCR	NR1H3	SREBF2	
CYP2C19	SLC6A4	NR1I3	NR1H2	DHCR7	NR3C1	SHH	IL2	ALDH2	
PPARA	CFTR	MMP1	MAPK10	MAP2K1	HSP90AA1	MMP7	ALPL	PIK3CA	
FGFR1	FLT1	TNF	PNP						

**Figure 4.** Venny diagram of related targets of XBS and liver injury.

### 3.4. Construction of drug-component-target network diagram

Through Cytoscape 3.9.1, we constructed a network diagram of the active components of XBS and their therapeutic targets for liver injury (**Figure 5**). In the diagram, red diamonds represented gene targets. Orange squares represented the active components of Radix Glycyrrhizae, and blue hexagons represented the active components of Cortex Mori, along with green circles representing the active components of Cortex Lycii. Yellow V-shapes represented the components shared by the three Chinese herbs. The network contained 196 nodes and 1537 edges. Through analysis, we found that the compounds with BC, CC, and Degree values greater than their average values in the top five were MOL000098 (quercetin), MOL000239 (jaranol), MOL000354 (isorhamnetin), MOL000359 (beta-sitosterol), and MOL000422 (kaempferol) (**Table 3**). These five components had significant influence in the drug-component-target network diagram. Therefore, the treatment of liver injury with XBS was a synergistic effect of multiple components.



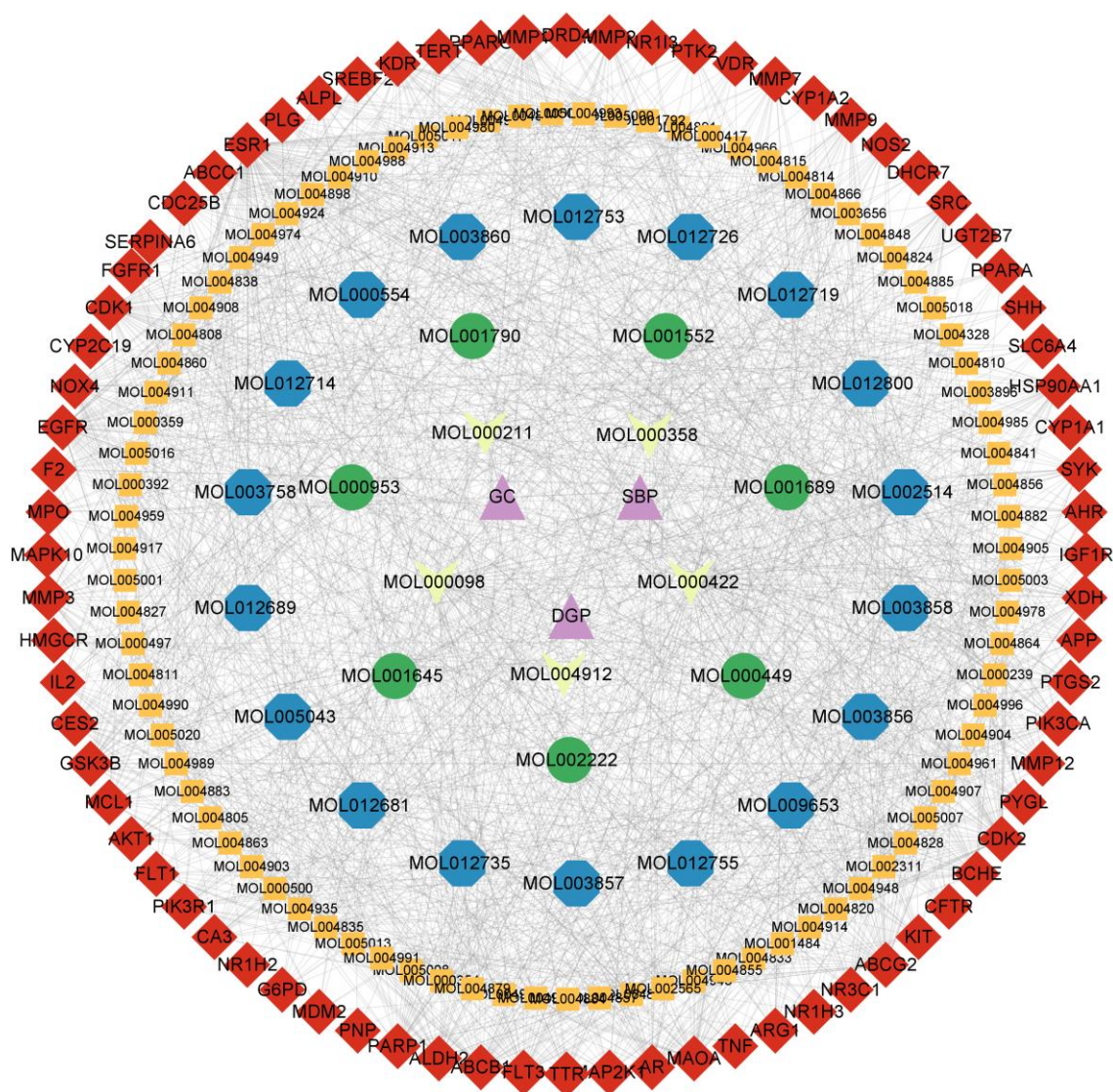


**Figure 5.** Drug-component-target network diagram.

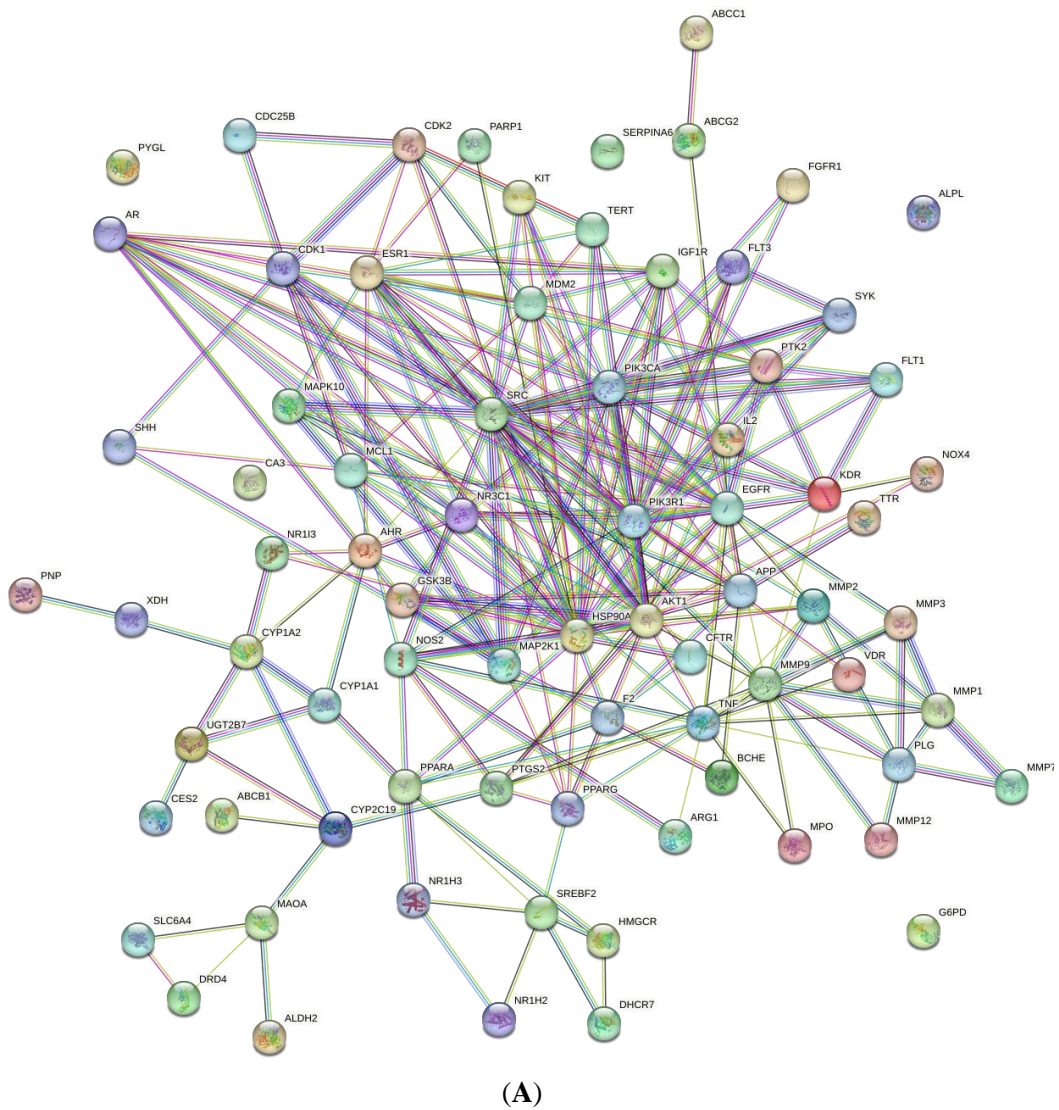
**Table 3.** Compounds with BC, CC, and degree values greater than their average values in the top five of the target gene count of XBS for liver injury.

MOL ID	Name	Degree	Betweenness Centrality	Closeness Centrality
MOL000098	quercetin	38	0.01	0.41
MOL000239	jaranol	23	0.01	0.44
MOL000354	isorhamnetin	35	0.02	0.45
MOL000359	beta-sitosterol	20	0.03	0.41
MOL000422	kaempferol	42	0.01	0.42

### 3.5. Protein interaction analysis and visualization

The 76 intersection targets of XBS and liver injury were imported into the STRING database to construct a PPI network diagram, which was then input into cytoscape 3.9.1 software for visualization (**Figure 6**). Through analysis, the top five key targets with the BC, CC, and Degree values of XBS in treating liver injury all

greater than their average values were HSP90AA1, SRC, EGFR, AKT1, and PIK3R1 (Table 4).



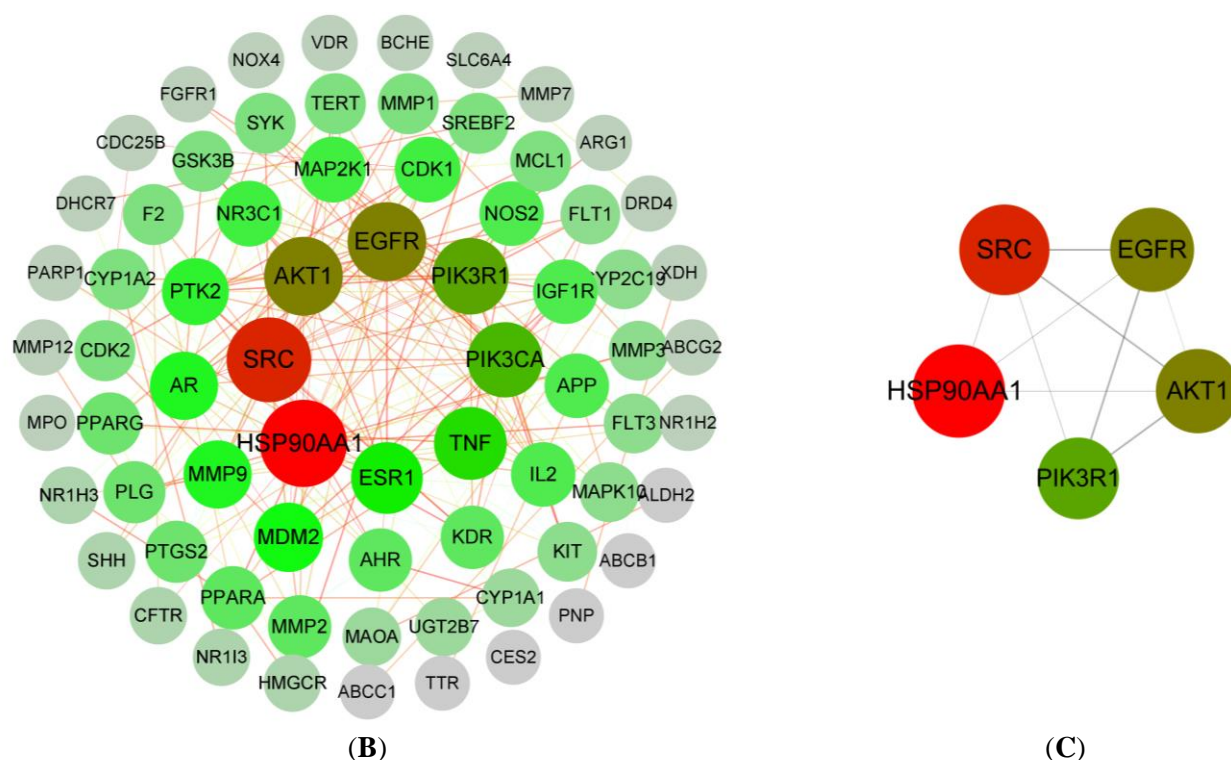


**Figure 6.** Protein-protein interaction (PPI) network of overlapping targets between XBS and liver injury. (A) Initial PPI network diagram; (B) Optimize PPI network; (C) Core PPI network.

**Table 4.** The top five key targets with the BC, CC, and degree values of XBS in treating liver injury all greater than their average values.

Name	Betweenness Centrality	Closeness Centrality	Degree
HSP90AA1	0.18	0.50	28.00
SRC	0.13	0.50	26.00
EGFR	0.15	0.48	21.00
AKT1	0.08	0.48	21.00
PIK3R1	0.03	0.42	19.00

### 3.6. GO function and KEGG pathway enrichment analysis

To elucidate the mechanism by which XBS treated liver injury, we performed GO function enrichment analysis (**Figure 7**) and KEGG pathway enrichment analysis (**Figure 8**) on the key targets using the David database. The x-axis in **Figure 7** represented the distinct names of biological processes, cellular components, and molecular functions, whereas the y-axis represented the enrichment score meaning the negative logarithm of the  $p$  value. The five key targets of XBS in treating liver injury were associated with multiple biological processes, mainly involving the following biological processes, as shown in **Figure 8**.

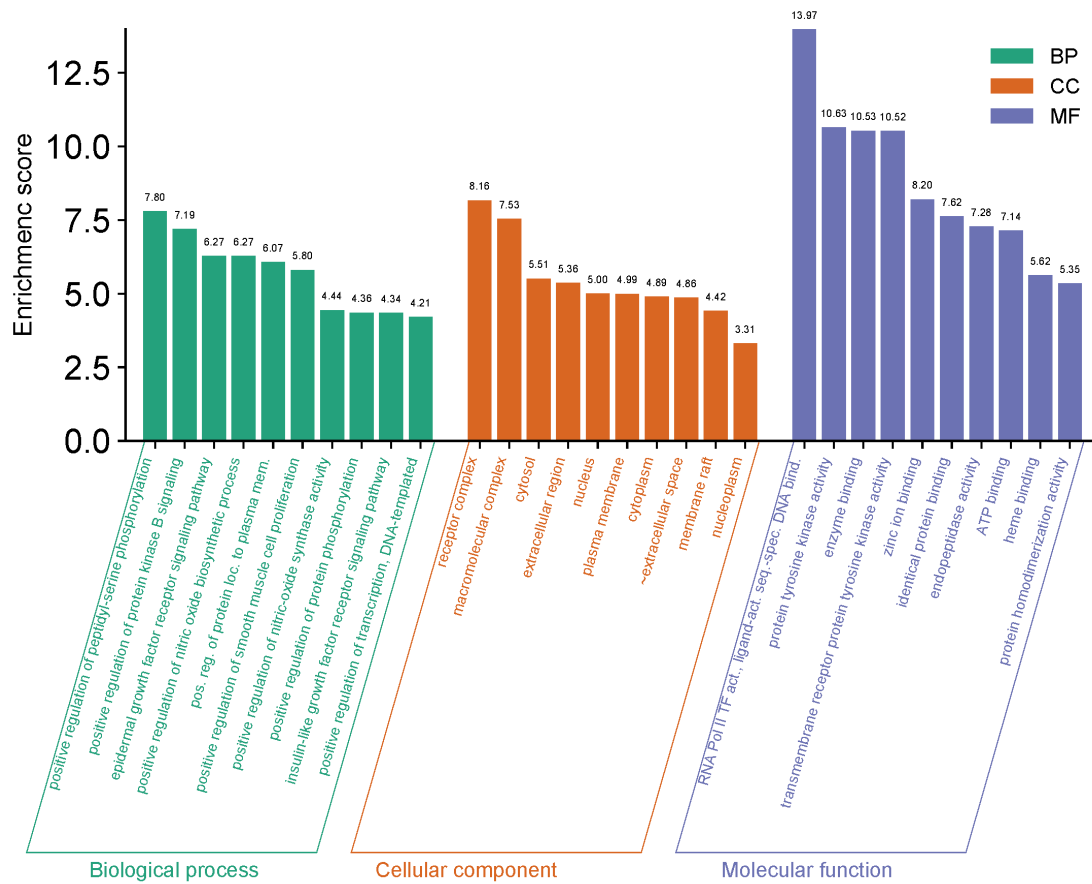


Figure 7. GO enrichment analysis.

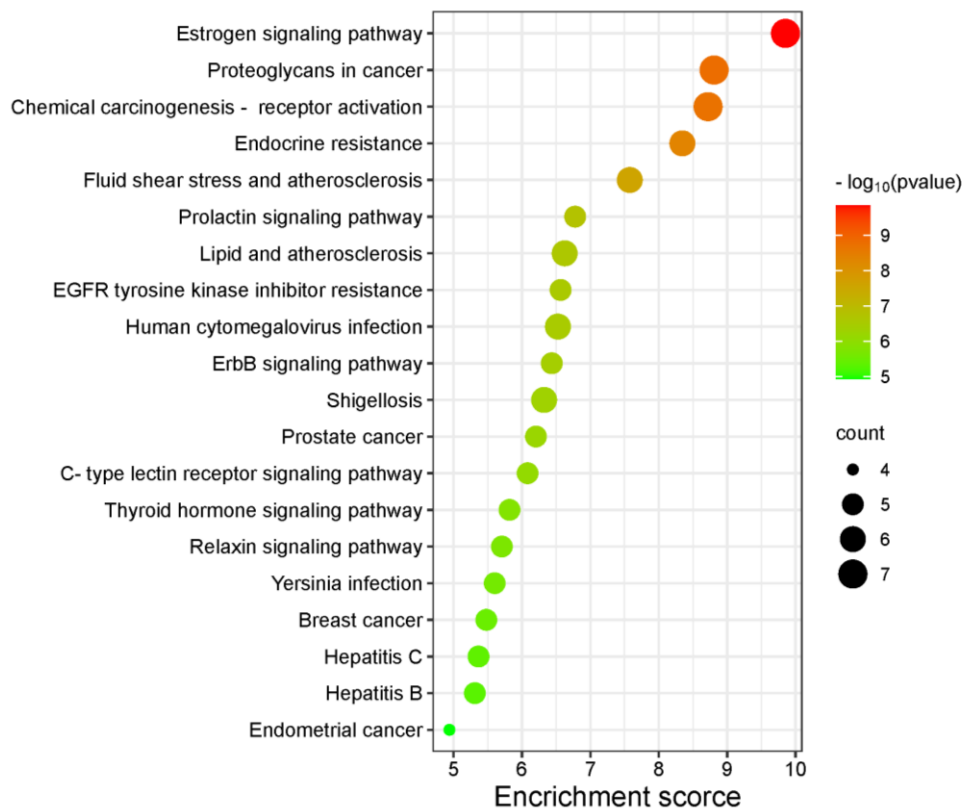


Figure 8. Bubble chart of pathway enrichment results.



### 3.8. Molecular docking verification

The main active components MOL000098 (quercetin), MOL000239 (jaranol), MOL000354 (isorhamnetin), MOL000359 (beta-sitosterol), and MOL000422 (kaempferol) in XBS were chosen to dock with the 5 key targets. The binding energies were presented in **Table 6** and **Figure 10**. Furthermore, PyMOL software was utilized to visualize the interaction between the compound and the target (**Figure 11**). The docking outcomes revealed that, 18 out of the 25 docking instances exhibited binding energies ranging from  $-5$  kcal/mol to above  $-7$  kcal/mol, suggesting favorable binding activity between the compound and the target. Among these, 5 pairs demonstrated binding energies below  $-7$  kcal/mol, indicating robust binding activity. Notably, 92% of the compounds displayed good binding activity with the targets, validating the prediction results.

**Table 6.** Molecular docking binding energy of active ingredients and targets.

MOL ID	Compound	Target	Binding energy/ (kcal · mol <sup>-1</sup> )
MOL000098	quercetin	EGFR	-6.25
		AKT1	-5.87
		PIK3R1	-5.34
		PIK3CA	-5.88
		ESR1	-4.68
MOL000239	Jaranol	EGFR	-7.62
		AKT1	-5.96
		PIK3R1	-5.32
		PIK3CA	-5.45
		ESR1	-7.27
MOL000354	isorhamnetin	EGFR	-6.25
		AKT1	-5.55
		PIK3R1	-5.43
		PIK3CA	-3.88
		ESR1	-6.61
MOL000359	beta-sitosterol	EGFR	-6.15
		AKT1	-7.58
		PIK3R1	-7.01
		PIK3CA	-5.34
		ESR1	-8.49
MOL000422	kaempferol	EGFR	-6.23
		AKT1	-6.11
		PIK3R1	-5.4
		PIK3CA	-5.28
		ESR1	-5.94

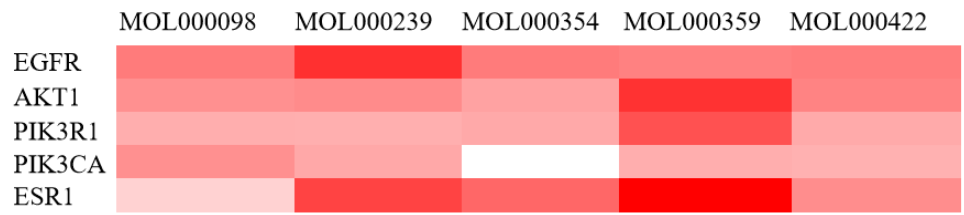
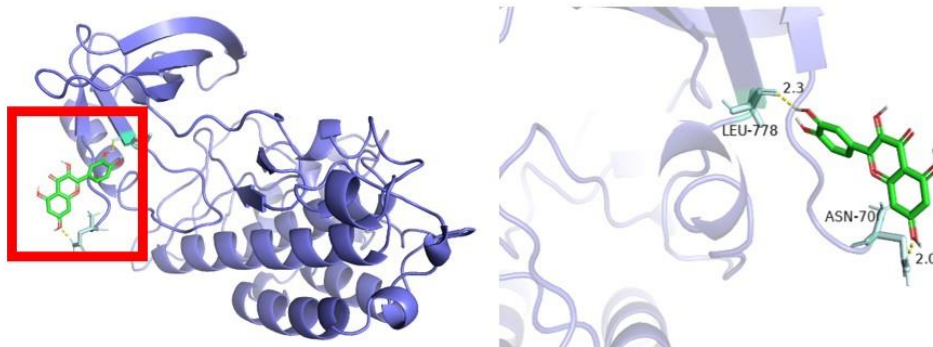
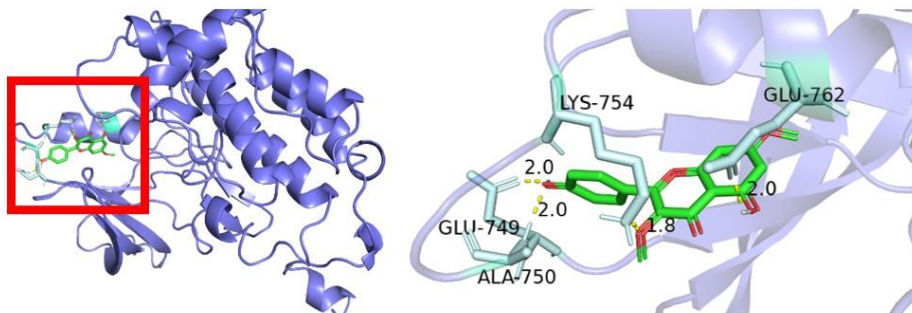


**Figure 10.** Molecular docking bond energy heat map.



(A)



(B)

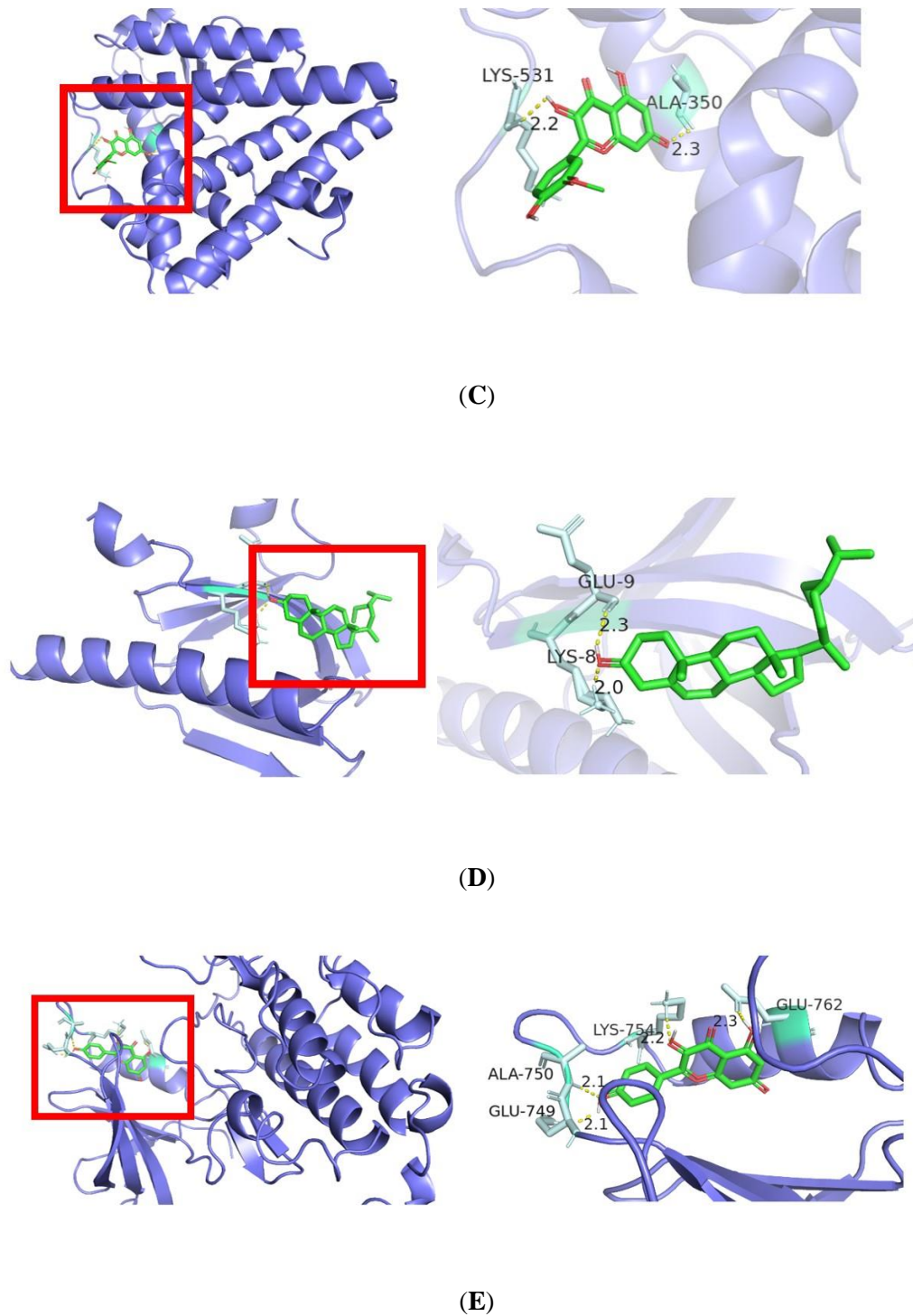


**Figure 11.** Molecular docking diagram. (A) Quercetin-EGF; (B) Jaranol- EGFR; (C) Isorhamnetin-ESR1; (D) Beta-sitosterol-AKT1; (E) Kaempferol- EGFR.

#### 4. Discussion

Liver injury is a disease caused by various reasons, represented by abnormal liver function [19]. It is related to many pathogenic mechanisms and presents a trend of high incidence rate and difficult cure, further affecting human life and health [20].



Acute liver injury is an acute inflammatory disease caused by viral hepatitis, drugs, toxins, and liver ischemia [21]. At present, effective treatment methods remain limited, mainly using liver protective drugs, such as pancreatic enzyme inhibitors, to enhance liver regeneration. Therefore, it is necessary to develop therapeutic drug on acute liver injury with less side effect.

XBS consists of Cortex Mori, cortex lycii, and radix glycyrrhizae and has the functions of relieving heat, reducing inflammation, resisting pathogenic microorganisms, and removing phlegm and relieving cough [22]. ALT and AST are two types of transaminases that exist in liver cells. Under normal circumstances, they exist in liver cells with low concentrations in the blood. If liver cells are injured, these two enzymes can be liberated into the bloodstream, causing elevated concentrations of ALT and AST. After treatment with XBS, the statistically significant difference was observed in the results. Specifically, the mice in the treatment group exhibited notably lower levels of AST and ALT, thereby confirming the therapeutic efficacy of XBS in CCl<sub>4</sub>-induced acute liver injury.

In the present study, the main active components in XBS screened by network pharmacology are quercetin,  $\beta$ -sitosterol, galangin, isorhamnetin, and kaempferol. Quercetin is a natural plant flavonoid whose biological activity has been widely studied. It has been reported that quercetin enhances the anti-hepatocellular carcinoma effect of doxorubicin through the p53/Bcl-xl pathway, and can upregulate the expression of adiponectin (ADPN) in rats with nonalcoholic fatty liver disease, effectively improving liver function and reducing liver inflammation [23].  $\beta$ -sitosterol, a plant sterol, has immunomodulatory, antioxidant, antiviral, anti-inflammatory, and anti-tumor effects [24]. Kaempferol prevents liver cell damage from acute liver injury caused by acetaminophen, and the molecular mechanism is related to antioxidant stress, promoting acetaminophen metabolism and inhibiting inflammation [25]. Isorhamnetin has the good protective effect on liver cell injury caused by drugs, significantly increasing the survival rate of liver cells injured by acetaminophen and elevating the contents of glutathione and superoxide dismutase in liver injury models [26]. Galangin can control apoptosis and inflammation via enhancing anti-inflammatory cytokines synthesis, and alleviating gut microbiota disorder to protect liver tissue [27,28].

In addition, this study predicted 391 potential targets for Cortex Mori, 360 potential targets for cortex lycii, 789 potential targets for Radix Glycyrrhizae, and 1128 potential targets of XBS on liver injury through network pharmacology. 76 common targets were identified through the intersection of the Venn diagram. The common targets were utilized to construct and visualize the PPI network diagram and visualized. The analysis results obtained from visualization were intersected with the drug-component-target-pathway visualization analysis results, and the key targets for XBS in treating liver injury were confirmed to be AKT1, EGFR, ESR1, PIK3CA, PIK3R1. The results of molecular docking displayed good binding energy between the main active components and the key targets. Specifically, quercetin and EGFR are hydrogen bound via leucine (LEU) at 778, and asparagine (ASN) at 70, and the binding energy reached  $-6.25$ . Jaranol and EGFR binded though glutamic acid (GLU) at 749 and 762 sites, lysine (LYS) at 754 sites, and alanine (ALA) at 750 sites with hydrogen bonds, and the binding energy reached  $-7.62$ . Isorhamnetin and ESR1 were hydrogen

bonded at ALA-350 and LYS-531, and the binding energy reached  $-6.61$ . Beta-sitosterol and AKT1 were hydrogen bound via LYS at site 3 and GLU at site 9 with binding energy of  $-7.58$ . Kaempferol and EGFR were hydrogen bound at GLU-749, ALA-750, LYS-754 and GLU-762, and the binding energy reached  $-6.23$ . The above binding showed good activity, indicating that the active compounds may play a vital role in improving liver function through the above target proteins.

AKT1, PIK3CA, and PIK3R1 are mainly involved in the PI3K/AKT signaling pathway, which can be activated by a range of cellular stimuli or toxic insults. Studies have shown that PIK3CA can activate signal cascades related to cell growth, survival, proliferation, movement, and morphology. AKT1 regulates multiple processes including metabolism, growth, cell survival, proliferation, and angiogenesis [29,30]. Cao et al. have found that white Peony could treat lupus nephritis by influencing signaling pathways related to cancer, lipid metabolism, atherosclerosis, the advanced glycation end product (AGE)-receptor for AGE (RAGE) pathways, C-type lectin receptor, and nuclear factor (NF)-kappa B signaling pathways through AKT1, VEGFA, and JUN [31]. ESR1 has an important impact on the progression of liver injury. ESR, also known as estrogen receptor, has two isoforms: ESR1 and ESR2. Estrogen in liver tissue primarily binds to ESR1 to exert antioxidant effect that inhibits liver fibrosis, prevents lipid deposition in the liver and blood and hinders the conversion of astrocytes into myofibroblasts to further decline the development of cirrhosis. Abnormal ESR1 protein levels in liver tissue can promote liver injury and catalyze the development of various liver diseases [32]. The epidermal growth factor receptor (EGFR), a tyrosine kinase receptor, regulates gene expression and controls cell growth and differentiation. It is overexpressed in tumor tissues and promotes tumor cell proliferation, invasion, metastasis, and angiogenesis [33].

Additionally, through KEGG enrichment analysis, the mechanism of the effect on liver injury was also closely associated with various biological processes such as positive regulation of peptide serine phosphorylation, epidermal growth factor receptor signaling pathway, positive regulation of nitric oxide biosynthesis, positive regulation of protein membrane localization, and positive regulation of protein kinase B signaling; cellular components such as receptor complexes, macromolecular complexes, cytoplasm, and extracellular regions; and molecular functions, such as ligand-activated sequence-specific DNA binding, protein tyrosine kinases activity, kinase binding, tyrosine kinase activity of transmembrane receptor, RNA polymerase II transcription factor activity, and zinc ion binding.

## **5. Conclusion**

XBS had good therapeutic effect on liver injury, and its therapeutic effect on liver injury exerted through multiple pathways and targets. The core components in XBS were quercetin, galangin, isorhamnetin,  $\beta$ -sitosterol, and kaempferol, and key targets are AKT1, EGFR, ESR1, PIK3CA, PIK3R1. Furthermore, XBS restored liver function, and the pathways of XBS in treating liver injury mainly included positive regulation of peptide-serine phosphorylation, positive regulation of protein kinase B signaling, epidermal growth factor receptor signaling pathway, positive regulation of

protein membrane localization. These findings provided the theoretical foundation for the development and utilization of XBS in acute liver injury.

**Supplemental materials:** Supplementary **Table S1**. Thirty two compounds in Cortex Mori screened by “oral bioavailability” (OB)  $\geq$  30% and “drug likeness” (DL); Supplementary **Table S2**. Thirteen compounds in Radix Paeoniae Alba screened by “oral bioavailability” (OB)  $\geq$  30% and “drug likeness” (DL); Supplementary **Table S3**. Ninety-two compounds in Glycyrrhiza uralensis is screened by “oral bioavailability” (OB)  $\geq$  30% and “drug likeness” (DL).

**Author contributions:** Conceptualization, TH, HQ and XL; methodology, TH and HQ; software, YL; validation, TH, CY, YL, YM, RL, MS, QZ and CL; formal analysis, TH and YL; investigation, YL, YM and XL; resources, TH, CY and YL; data curation, TH, CY, YL, YM and CL; writing—original draft preparation, TH and YL; writing—review and editing, TH and CY; visualization, YL, YM, QZ and CL; supervision, HQ and XL; project administration, TH, CY, YL, HQ and XL; funding acquisition, CY and HQ. All authors have read and agreed to the published version of the manuscript.

**Funding:** This work was supported by Scientific and technological research projects in Henan Province (222102310374), Key Research Projects of Henan Higher Education Instituti (23B360007 and 21B310008), and Outstanding Young Teachers Program of Sanquan College of Xinxiang Medical University (SQ2023YQJH06).

**Ethical approval:** The study was conducted in accordance with the Declaration of Helsinki. The experimental procedures were approved by the Ethics Committee of the Experimental Animal Platform of Zhengzhou University School of Medical Sciences. The ethics approval number for this experiment is ZZU-LAC20230210.

**Conflict of interest:** The authors declare no conflict of interest.

## References

1. Okubo S, Miyamoto M, Ito D, Takami K, Ashida K. Albumin and apolipoprotein H mRNAs in human plasma as potential clinical biomarkers of liver injury: analyses of plasma liver-specific mRNAs in patients with liver injury. *Biomarkers*. 2016;21(4):353-62.
2. Zhao T, Yu Z, Zhou L, Wang X, Hui Y, Mao L, Fan X, Wang B, Zhao X, Sun C. Regulating Nrf2-GPx4 axis by bicyclol can prevent ferroptosis in carbon tetrachloride-induced acute liver injury in mice. *Cell Death Discov*. 2022 Sep 7;8(1):380.
3. Zhao CQ, Zhou Y, Ping J, Xu LM. Traditional Chinese medicine for treatment of liver diseases: progress, challenges and opportunities. *J Integr Med*. 2014 Sep;12(5):401-8.
4. Xiang D, Zou J, Zhu X, Chen X, Luo J, Kong L, Zhang H. Physalin D attenuates hepatic stellate cell activation and liver fibrosis by blocking TGF- $\beta$ /Smad and YAP signaling. *Phytomedicine*. 2020 Nov;78:153294.
5. Zhao A, Guo C, Wang L, Chen S, Xu Q, Cheng J, Zhang J, Jiang J, Di J, Zhang H, Chen F, Su J, Jiang L, Liu L, Liu Y, Liu A. Xiebai San alleviates acute lung injury by inhibiting the phosphorylation of the ERK/Stat3 pathway and regulating multiple metabolisms. *Phytomedicine*. 2024 Jun;128:155397.
6. Zhao A, Su J, Xu Q, Zhang J, Jiang J, Chen S, Cheng J, Chen C, Wang L, Di J, Liu X, Jiang L, Liu L, Liu Y, Liu A, Guo C. Elucidation of anti-pneumonia pharmacodynamic material basis and potential mechanisms of Xiebai San by combining spectrum-efficacy relationship and surface plasmon resonance. *J Ethnopharmacol*. 2024 Dec 5;335:118609.
7. Jiashuo WU, Fangqing Z, Zhuangzhuang LI, Weiyi J, Yue S. Integration strategy of network pharmacology in Traditional Chinese Medicine: a narrative review. *J Tradit Chin Med*. 2022 Jun;42(3):479-486.

8. Wei Yuanyuan, Fan Yimeng, Yuan Yanyan, et al. Protective Effect of Aqueous Extract of Yinshanlian on Acute Liver Injury Induced by Carbon Tetrachloride in Mice[J]. *Acta Veterinaria et Zootechnica Sinica*, 2022, 53(07): 2333-2342.
9. RU J, LI P, WANG J, et al. TCMSP: a database of systems pharmacology for drug discovery from herbal medicines [J]. *J Cheminform*, 2014, 6: 13.
10. KIM S, CHEN J, CHENG T, et al. PubChem 2023 update [J]. *Nucleic Acids Research*, 2022, 51(D1): D1373-D80.
11. DAINA A, MICHIELIN O, ZOETE V. SwissTargetPrediction: updated data and new features for efficient prediction of protein targets of small molecules [J]. *Nucleic Acids Research*, 2019, 47(W1): W357-W64.
12. Luo W, Deng J, He J, Yin L, You R, Zhang L, Shen J, Han Z, Xie F, He J, Guan Y. Integration of molecular docking, molecular dynamics and network pharmacology to explore the multi-target pharmacology of fenugreek against diabetes. *J Cell Mol Med*. 2023 Jul;27(14):1959-1974.
13. Liu T, Wang J, Tong Y, Wu L, Xie Y, He P, Lin S, Hu X. Integrating network pharmacology and animal experimental validation to investigate the action mechanism of oleanolic acid in obesity. *J Transl Med*. 2024 Jan 21;22(1):86.
14. Ji L, Song T, Ge C, Wu Q, Ma L, Chen X, Chen T, Chen Q, Chen Z, Chen W. Identification of bioactive compounds and potential mechanisms of scutellariae radix-coptidis rhizoma in the treatment of atherosclerosis by integrating network pharmacology and experimental validation. *Biomed Pharmacother*. 2023 Sep;165:115210.
15. Yu S, Fan C, Li Y, Pei H, Tian Y, Zuo Z, Wang Z, Liu C, Zhao X, Wang Z. Network pharmacology and experimental verification to explore the anti-migraine mechanism of Yufeng Ningxin Tablet. *J Ethnopharmacol*. 2023 Jun 28;310:116384.
16. Althagafy HS, Ali FEM, Hassanein EHM, Mohammedsalem ZM, Kotb El-Sayed MI, Atwa AM, Sayed AM, Soubh AA. Canagliflozin ameliorates ulcerative colitis via regulation of TLR4/MAPK/NF- $\kappa$ B and Nrf2/PPAR- $\gamma$ /SIRT1 signaling pathways. *Eur J Pharmacol*. 2023 Dec 5;960:176166.
17. Liu T, Li Y, Wang L, Zhang X, Zhang Y, Gai X, Chen L, Liu L, Yang L, Wang B. Network pharmacology-based exploration identified the antiviral efficacy of Quercetin isolated from mulberry leaves against enterovirus 71 via the NF- $\kappa$ B signaling pathway. *Front Pharmacol*. 2023 Sep 19;14:1260288.
18. Noor F, Asif M, Ashfaq UA, Qasim M, Tahir Ul Qamar M. Machine learning for synergistic network pharmacology: a comprehensive overview. *Brief Bioinform*. 2023 May 19;24(3):bbad120.
19. Liu P, Hao J, Zhao J, Zou R, Han J, Tian J, Liu W, Wang H. Integrated Network Pharmacology and Experimental Validation Approach to Investigate the Therapeutic Effects of Capsaicin on Lipopolysaccharide-Induced Acute Lung Injury. *Mediators Inflamm*. 2022 Jan 30;2022:9272896.
20. Pu S, Zhang J, Ren C, Zhou H, Wang Y, Wu Y, Yang S, Cao F, Zhou H. Montelukast prevents mice against carbon tetrachloride- and methionine-choline deficient diet-induced liver fibrosis: Reducing hepatic stellate cell activation and inflammation. *Life Sci*. 2023 Jul 15;325:121772.
21. Xian S, Yang Y, Nan N, Fu X, Shi J, Wu Q, Zhou S. Inhibition of mitochondrial ROS-mediated necroptosis by *Dendrobium nobile* Lindl. alkaloids in carbon tetrachloride induced acute liver injury. *J Ethnopharmacol*. 2024 Aug 10;330:118253.
22. Chen M, Zhong G, Liu M, He H, Zhou J, Chen J, Zhang M, Liu Q, Tong G, Luan J, Zhou H. Integrating network analysis and experimental validation to reveal the mitophagy-associated mechanism of Yiqi Huoxue (YQHX) prescription in the treatment of myocardial ischemia/reperfusion injury. *Pharmacol Res*. 2023 Mar;189:106682.
23. Zhang Q, Gao Y, Wang Y, Liu DH, Liu CF, Zhong LY, Liang J, Tian WW, Hong TT, Bai J, DU SY. [Particle size of “Cuo San” of famous classical formulas and decoction process with Xiebai San for example]. *Zhongguo Zhong Yao Za Zhi*. 2020 Feb;45(4):878-883. Chinese.
24. Khan Z, Nath N, Rauf A, Emran TB, Mitra S, Islam F, Chandran D, Barua J, Khandaker MU, Idris AM, Wilairatana P, Thiruvengadam M. Multifunctional roles and pharmacological potential of  $\beta$ -sitosterol: Emerging evidence toward clinical applications. *Chem Biol Interact*. 2022 Sep 25;365:110117.
25. Li H, Weng Q, Gong S, Zhang W, Wang J, Huang Y, Li Y, Guo J, Lan T. Kaempferol prevents acetaminophen-induced liver injury by suppressing hepatocyte ferroptosis via Nrf2 pathway activation. *Food Funct*. 2023 Feb 21;14(4):1884-1896.
26. Yang X, Wang H, Shen C, Dong X, Li J, Liu J. Effects of isorhamnetin on liver injury in heat stroke-affected rats under dry-heat environments via oxidative stress and inflammatory response. *Sci Rep*. 2024 Mar 29;14(1):7476.
27. Thapa R, Afzal O, Alfawaz Altamimi AS, Goyal A, Almalki WH, Alzarea SI, Kazmi I, Jakhmola V, Singh SK, Dua K, Gilhotra R, Gupta G. Galangin as an inflammatory response modulator: An updated overview and therapeutic potential. *Chem Biol Interact*. 2023 Jun 1;378:110482.

28. Zhao Y, Li B, Deng H, Zhang C, Wang Y, Chen L, Teng H. Galangin Alleviates Alcohol-Provoked Liver Injury Associated with Gut Microbiota Disorder and Intestinal Barrier Dysfunction in Mice. *J Agric Food Chem*. 2024 Oct 9;72(40):22336-22348.
29. Peng Y, Zhu G, Ma Y, Huang K, Chen G, Liu C, Tao Y. Network Pharmacology-Based Prediction and Pharmacological Validation of Effects of Astragali Radix on Acetaminophen-Induced Liver Injury. *Front Med (Lausanne)*. 2022 Jul 4; 9: 697644.
30. Hu B, Zou T, Qin W, Shen X, Su Y, Li J, Chen Y, Zhang Z, Sun H, Zheng Y, Wang CQ, Wang Z, Li TE, Wang S, Zhu L, Wang X, Fu Y, Ren X, Dong Q, Qin LX. Inhibition of EGFR Overcomes Acquired Lenvatinib Resistance Driven by STAT3-ABCB1 Signaling in Hepatocellular Carcinoma. *Cancer Res*. 2022 Oct 17;82(20):3845-3857.
31. Cao Y, Wang C, Dong L. Exploring the Mechanism of White Peony in the Treatment of Lupus Nephritis Based on Network Pharmacology and Molecular Docking. *Arch Esp Urol*. 2023 Mar;76(2):123-131.
32. González L, Díaz ME, Miquet JG, Sotelo AI, Dominici FP. Growth Hormone Modulation of Hepatic Epidermal Growth Factor Receptor Signaling. *Trends Endocrinol Metab*. 2021 Jun;32(6):403-414.
33. Kamei H, Onishi Y, Nakamura T, Ishigami M, Hamajima N. Role of cytokine gene polymorphisms in acute and chronic kidney disease following liver transplantation. *Hepatol Int*. 2016 Jul;10(4):665-72.